JOURNAL OF THERMOPHYSICS AND HEAT TRANSFER
Vol. 15, No. 1, January–March 2001

Thermal Plume Turbulent Enhancement, Reverse Transition, and Relaminarization in Stably Stratified Enclosure

Katsuhisa Noto,* Yoshiharu Meguro,† and Tsuyoshi Nakajima†
Kobe University, Nada, Kobe 657-8501, Japan

For a thermally buoyant plume in stably stratified ambient air at the heating rate $Q = 0.32$–27.8 W/m, flow patterns are visualized experimentally, the time-dependent temperature is measured, and the power spectrum density (PSD) is obtained. The PSDs have gradients with $-\frac{9}{2}$ and -8.0 in the laminar state and $-\frac{5}{3}$ and -3.0 in the turbulent state. In addition, the frequency band of turbulence is higher than that of the swaying motion, where stable stratification increases the swaying frequency by 37% at the stratification degree $st = 0.3$ K/cm. Flow regions of the laminar, transitional, and turbulent states at any location are determined. When the flow regions are plotted on visualization photographs, the turbulent transition, reverse transition, and relaminarization are specified and compared with unstratified results. As a result, stable stratification enhances the turbulence generation below the plume front, suppresses turbulence near and above the plume front, and leads to reverse transition and relaminarization, which never occur in an unstratified ambient and characterize the plume in a stratified ambient. The Grashof number Gr_s ($= 1.32 \times 10^8 Ra_B^{1.62}$) for the beginning of the turbulent transition increases with an increase of Q, where Ra_B is the Rayleigh number proportional to Q. The transitional or the turbulent state occurs at larger than the critical Rayleigh number Ra_{Bs} ($= 4.28 \times 10^8$–9.15×10^8) or Ra_{Be} ($= 1.68 \times 10^9$–2.87×10^9) on the midplane.

Nomenclature

B	=	horizontal length between wire and side wall, $B_0/2$, mm
B_0	=	enclosure width, 800 mm
$C(\tau_s)$	=	autocorrelation function, $\overline{t(t_t)t(t_t+\tau_s)}$, K^2
d	=	diameter of heat source, 0.435 mm
f	=	frequency, Hz
Gr_x	=	local Grashof number, $x^3 g\beta Q/\nu^2\lambda Pr$
g	=	gravitational acceleration, m/s^2
H	=	enclosure height, 1000 mm
H_0	=	vertical length between wire and bottom surface, 400 mm
I	=	electric current, A
i	=	time number of time-series data; imaginary unit
L	=	length of heat source, 550 mm
N	=	number of sampling data
$P(f)$	=	power spectrum density (PSD), K^2 s

$$\int R(\tau)\exp(-i2\pi f\tau)\,\mathrm{d}\tau$$

Pr	=	Prandtl number
Q	=	convective heating rate per unit length of heat source, $Q_t - Q_r$, W/m
Q_r	=	radiative heating rate per unit length of heat source, $\varepsilon_m\sigma_s\pi d(T_w^4 - T_\infty^4)$, W/m
Q_t	=	total heating rate generated per unit length of heat source, IV/L, W/m
$R(\tau_s)$	=	autocorrelation coefficient (ACC), $C(\tau_s)/C(0)$
Ra_B	=	Rayleigh number, $B^3 g\beta Q/\lambda\nu^2$
Re_{fB}	=	frequency Reynolds number, fB^2/ν
S	=	power spectrum density normalized by temperature variance, $P(f)/\sigma^2$, s
st	=	stratification degree, $(\mathrm{d}T_a/\mathrm{d}X)_\infty$, K/cm
T	=	time-averaged temperature, $(\Sigma t_i)/N$, K
T_a	=	stratified air temperature, K
t	=	instantaneous temperature, $T + t'$, K
t_t	=	time, s
t'	=	temperature fluctuation, $t - T$, K
V	=	voltage difference between ends of heat source, V
W	=	enclosure depth, 800 mm
X	=	vertical coordinate from wire center, mm
Y	=	horizontal coordinate perpendicular to wire axis from wire center, mm
Z	=	horizontal coordinate along wire axis from center of enclosure width, mm
β	=	volumetric coefficient of thermal expansion, $1/T_\infty$, 1/K
ε_m	=	emissivity of heat source
λ	=	thermal conductivity, W/mK
ν	=	kinematic viscosity, m^2/s
σ	=	standard deviation of temperature, $[(\Sigma t_i - T)^2/N]^{1/2}$, K
σ_s	=	Stefan–Boltzmann constant, W/m^2 K^4
τ	=	swaying period, Hz
τ_s	=	time lag, s

Subscripts and Superscript

e	=	at beginning of turbulent state on midplane
i	=	at i of time-series data
s	=	at beginning of transitional state on midplane
w	=	on heat source
∞	=	far away from plume
-	=	time average

Received 1 February 1999; revision received 18 August 2000; accepted for publication 24 August 2000.

*Department of Mechanical Engineering; noto@mech.kobe-u.ac.jp.
†Department of Mechanical Engineering.

Introduction

THE plume above a horizontal line heat source in an unstratified ambient has been studied by many researchers.[1–5] Noto[3] and Noto et al.[5] elucidated the swaying frequency, the laminar characters, and the turbulent transition in the plume. Because the plume sways[1–5] naturally without an artificial disturbance, the turbulent plume is time dependent due to both turbulence and the swaying motion and is very complicated. Also, the natural convection in a

stably stratified fluid has been studied by many researchers.[6–10] In particular, the buoyant plume in a stably stratified ambient is very important not only in thermofluid dynamics but also as atmospheric phenomena, for example, the heat island plume[11] and the stellar envelope convection.[12]

The flow state, that is, laminar, transitional, or turbulent, in the plume in an unstratified ambient was determined macroscopically and qualitatively by the turbulent burst[1] and the Mach–Zehnder visualization[2] and determined exactly by the power spectrum density (PSD).[5] However, a method for determining a flow state in stable stratification has not been developed because it is not clear whether the existing methods[1,2,5] are or are not applicable to it. As a result, reverse transition with turbulence suppression and relaminarization without any turbulence in a stratified ambient have not been specified. Furthermore, the stably stratified fluid layer without a plume has been studied by only Narasimha and Sreenivasan[13] and Tritton,[14] who said that stable stratification qualitatively and roughly suppresses turbulence, and Lumley,[15] who discussed whether or not the PSD gradient is -3.0 in the inertia-diffusive subrange. That is, at present, a mechanism for and details of turbulence suppression due to stable stratification are as yet not clear, and the PSD gradient -3.0 in the inertia-diffusive subrange has not been validated experimentally.

For the plume in a stratified ambient, there are important questions that have not been answered:

1) How is a flow pattern, that is, streaklines, transformed by stable stratification?

2) Can we determine a flow state at any location with two different kinds of time-dependent motions, one turbulence and the other a swaying motion?

3) What is an effect of stable stratification on turbulent transition?

The purpose of the present study is, therefore, as follows:

1) The plume pattern in a stably stratified ambient is elucidated by flow visualization.

2) The time-dependent temperature is measured, and PSDs are obtained by the statistical analysis of the measured temperature.

3) The obtained PSDs are discussed: Whether the flow states can be determined or not is elucidated and regions of the flow state determined in a stably stratified ambient are compared with those in an unstratified ambient.

4) The effects and flow physics of stable stratification on the generation or the suppression of turbulence and turbulent transition are made clear.

Experimental Apparatus and Methods

Formation of Stable Stratification and Plume Generation

The experimental apparatus and the measuring system are shown in Fig. 1. To exclude disturbances from the ambient, stably stratified air was formed in the enclosure (800×800 mm, $B_0 \times W$ in Fig. 1) square cross section, 1000 mm height H, with the ceiling H_v, with high temperature by electrically heating, and the bottom surface C_v, with low temperature by cooling with ice and water. Air at the atmospheric pressure filled the enclosure, and the stably stratified temperature of the air was independent of time and the Y and Z directions. The enclosure volume, 0.640 m^3 in the present experiment, was smaller than the 1.12 m^3 volume in Ref. 7, nearly equal to 0.648 m^3 volume in Refs. 8 and 9, and larger than the 0.0613 m^3 volume in Ref. 6, 0.55 m^3 volume in Ref. 2, and 0.51 m^3 volume in Ref. 1. The volume in Ref. 7 is very large because of water in the enclosure. However, for air, the volume in the present experiment is rather large. A plume was generated from a nichrome heated wire, H_w, $d = 0.435$ mm in diameter, and $L = 550$ mm long, placed 400 mm, H_0, above the bottom surface. The wire was electrically heated for generating a thermally buoyant plume. The convective heating rate Q per unit length of heat source was obtained by $Q = Q_t - Q_r$.

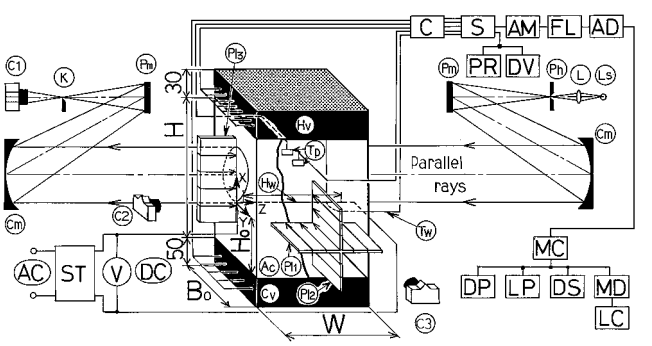

AC: Alternative Current
AM: Amplifier
C1, C2, C3: Camera
DC: Direct Current
DV: Digital Voltmeter
Ho: Distance from Bottom to Wire
LC: Large Scale Computer
P11, P12, P13: Plane Ray
S : Switch
Tw: Thermocouple on Wire
Ac: Acrylate Resin
B : Enclosure Breadth
Cm: Concave Mirror
DP: Display
FL: Lowwpass Filter
Hv: Heated Vessel
K : Knife Edge
LP: Line Printer
MD: Modem
Pm: Plane Mirror
ST: Stabilizer
V V: Voltmeter
AD: AD Converter
C : Compensator
Cv: Cooled Vessel
DS: Disk
H : Enclosure Height
Hw: Heated Wire
L : Condensed Lens
MC: Micro Computer
Ph: Pin Hole
PR: Pen Recorder
Tp: Thermocouple in Plume
W : Enclosure Width

Fig. 1 Experimental apparatus and measuring system.

Plume Visualization

First, smoke from an incense stick as a tracer filled the enclosure, and then the sheet light $P1_3$ or $P1_1$ was applied either vertically at $Y = 0$ or horizontally along the wire axis to examine the end effect of the wire or the meandering motion defined as the oscillation in the Z direction. Second, the sheet light $P1_2$ was vertically applied perpendicular to the wire axis to visualize a plume pattern and the swaying motion defined as the oscillatory motion in the X–Y plane due to a natural disturbance. Third, a small vessel filled with smoke was placed below the wire. The smoke temperature in the vessel was equal to the stratified fluid temperature around the vessel. The smoke issued from the vessel at a very slow velocity and rose upward by the entrainment of the plume in $X < 0$. Then the smoke entered the plume at $0 < X$. Thus, the plume motion was visualized. Fourth, an experiment was performed to examine the effect of smoke on the resulting physics of the flow because close attention should be paid not to confuse a vortex as a wreck motion of the smoke tracer. As a result, a large number of photographs and video tapes were obtained and discussed, and the smoke effect on the resulting physics of the flow was found to be negligible. Furthermore, the plume temperature was visualized by the schlieren method (C_1–Ls). Flow visualization results of the plume agreed well with those in the temperature visualization, the time record of the temperature, and the spectrum shown later.

Temperature Measurement and Acquisition of Time-Series Data of Temperature

Thermocouples T_p, 25.0–100.0 μm in diameter, were used to measure the time-dependent temperature. The time constant of the thermocouple is larger than 25 Hz and is sensitive and reasonable for measuring the time-dependent temperature because the dominant frequency of the plume temperature is less than 1.0 Hz. The output from the thermocouple reaches an A/D board through an amplifier and a low-pass filter and was digitized. Discretized time-series data of the temperature were recorded on a floppy disk on a microcomputer system. The time and the number for sampling of the digitized temperature were determined as discussed by Noto and Matsumoto.[16] The Nyquist frequency in the present sampling process was much larger than the plume frequency. The present sampling is, therefore, reasonable for the spectrum analysis and the discussion of the plume motion with both turbulence and a swaying motion. The temperature resolution was smaller than 0.1 K, which is sufficient for accuracy of the statistical analysis.

Statistical and Spectrum Analysis

Time-series data of the digitized temperature were analyzed statistically; the autocorrelation coefficient (ACC), probability density function (PDF), and PSD of the plume temperature were obtained by the maximum entropy method[17] for a time longer than a swaying period.

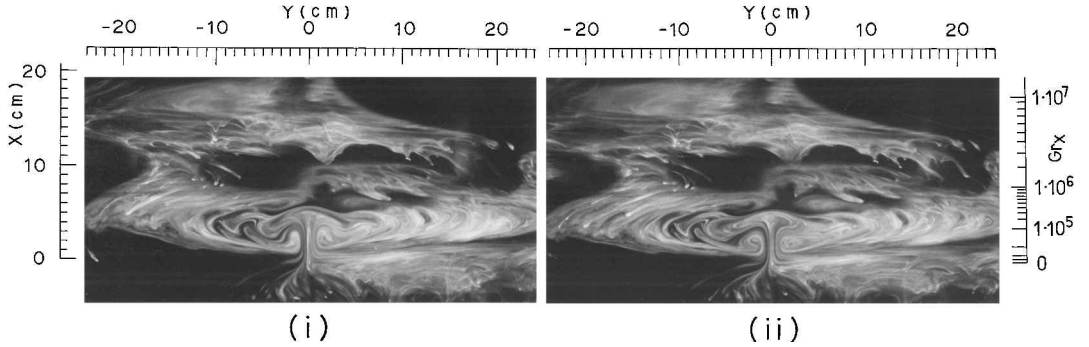

a) $Q = 0.32$ W/m (extremely low heating rate)

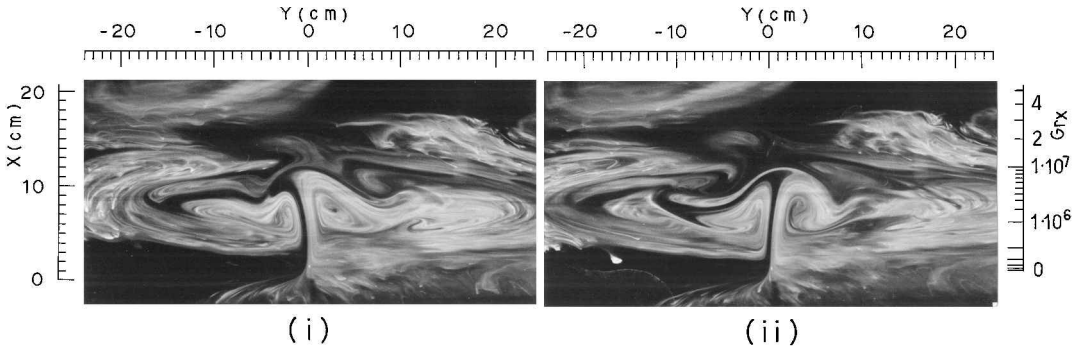

b) $Q = 1.30$ W/m (low heating rate)

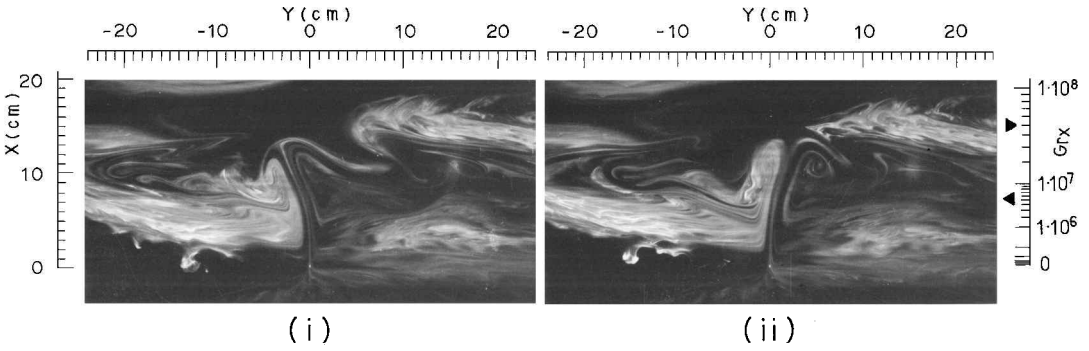

c) $Q = 2.75$ W/m (moderate heating rate)

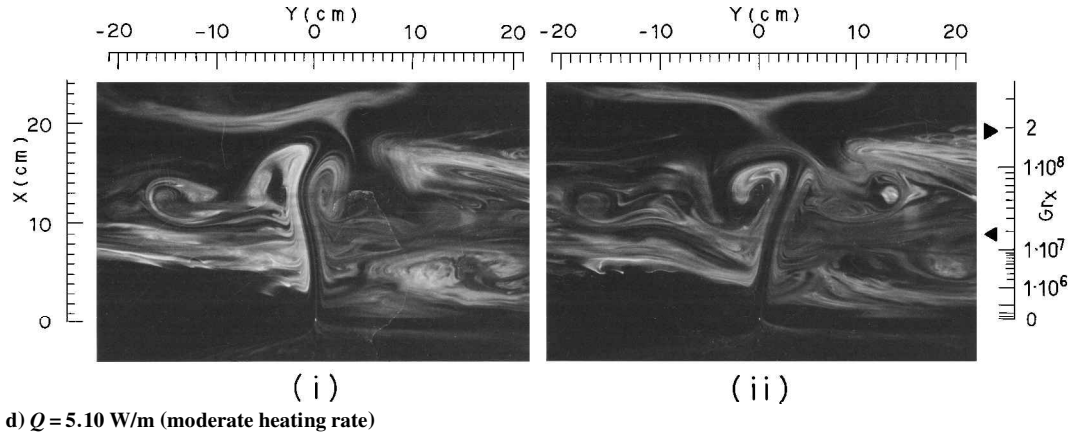

d) $Q = 5.10$ W/m (moderate heating rate)

Fig. 2 Instantaneous flow pattern at $st = 0.3$ K/cm.

Validity of Plume Formation, Visualization, Measurement, and Statistical Analysis

The plume pattern in a stably stratified ambient obtained by the present method agrees qualitatively with that obtained by Giovannoi,[7] who used a heated plate instead of a heated wire as a heat source. The time-averaged temperature obtained on the midplane at $st = 0$ K/cm agreed well with those obtained by Forstrom and Sparrow,[1] Bill and Gebhart,[2] and Noto[3] in the laminar region and those obtained by Rouse et al.[18] and Noto et al.[5] in the turbulent region, where st is the stratification degree defined as the ambient temperature gradient in the vertical direction. The PSDs obtained at $st = 0$ K/cm agreed well with previous results.[3,5] The swaying frequency determined by the dominant frequency of the plume PSD in a stratified ambient agreed well with that obtained by flow visualization. The formation of stably stratified air, plume generation, visualization methods, sensing, data transfer, acquisition of time-series data, statistical analysis, spectrum analysis, and results in the present study are, therefore, accurate and reasonable.

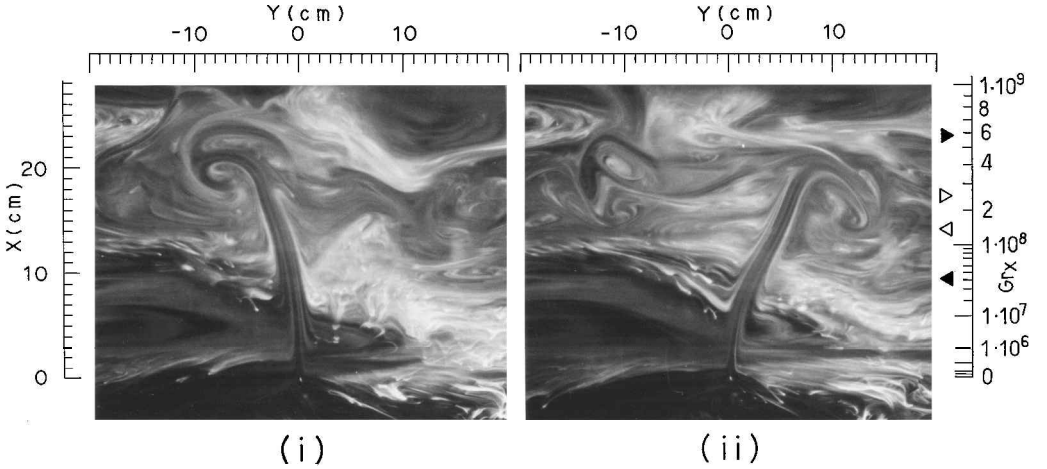

e) $Q = 8.73$ W/m (high heating rate)

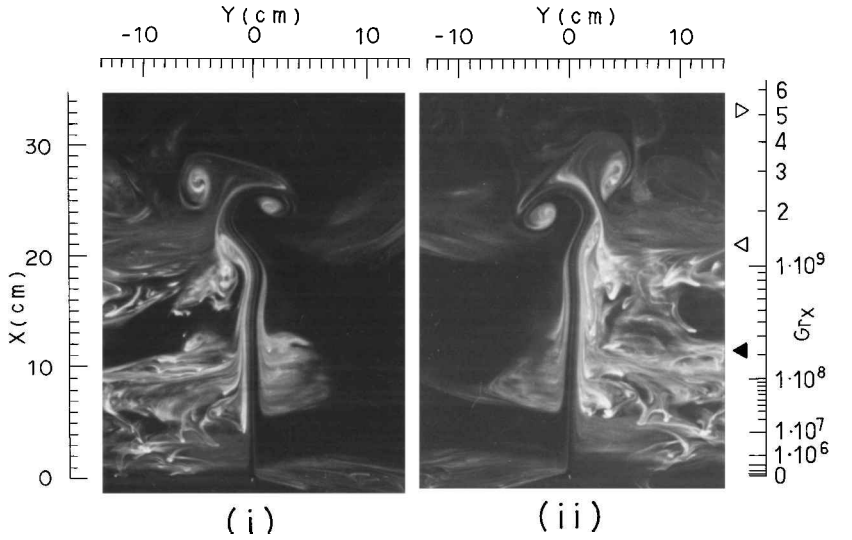

f) $Q = 27.8$ W/m (extremely high heating rate)

Fig. 2 Instantaneous flow pattern at $st = 0.3$ K/cm (continued).

Conditions of Stratification Degree and Heating Rate

The values of st are 0, 0.15, and 0.3 K/cm. $Q = 0.32$–27.8 W/m, where $Q = 0.32$ W/m is extremely low Q, 1.30 is low Q, 2.75 and 5.10 are moderate Q, 8.73 is high Q, and 27.8 is extremely high Q. Only results at $st = 0.3$ K/cm are shown later because results in the laminar region at $st = 0$ K/cm agreed well with the previous results[1–3,5] and results at $st = 0.15$ K/cm were distributed between those at $st = 0$ and 0.3 K/cm.

Plane Plume and Downflow Effect

Because the aspect ratio $L/d = 1264$ of the wire in the present experiment is larger than in Refs. 1 ($L/d = 249$) and 2 ($L/d = 741$), the plume in a stratified ambient was not axisymmetric but was plane as is the plume in an unstratified ambient.[19] By observation, the plume was found to rise vertically. The measured temperature did not vary to the Z direction in $-250 \leqq Z \leqq 250$ mm, where the plume was not affected by the end of the wire. At any Q, the meandering motion did not occur at $B_0 = 800$ mm, did occur at $B_0 = 600$, and became dominant with a decrease of B_0. At $B_0 = 800$ mm, the swaying motion occurred. The plume was time dependent but was a time-averaged two-dimensional plane in the whole region. The effect of the inevitable downflow on the plume motion in a stratified ambient was negligible. For the downflow, its region was near the midplane, and its velocity was very small at small Q. With increasing Q, its region moved to the neighborhood of the side walls, and its velocity became 5% of the plume velocity on the midplane.

Flow Pattern

Instantaneous plume patterns on the X–Y plane at different times obtained by flow visualization are shown in Fig. 2, where X and Grashof number Gr_x on the midplane are shown on the left and right sides, respectively. Physical properties are evaluated at the reference temperature $T_r = \{T_{CL} - 0.38(T_{CL} - T_\infty)\}$, where T_{CL} is the temperature on the midplane, and the symbols on the ordinate are shown in Table 1.

At $0.32 \leqq Q \leqq 27.8$ W/m, the plume patterns can be classified into four kinds: At $Q = 0.32$ W/m (Fig. 2a), the height is small, and the horizontal length between the wire and the plume side is large. The flow in Fig. 2a is called the fumigation flow. With an increase of Q, the plume pattern changes as follows: 1) fumigation flow (Figs. 2a and 2b), 2) mushroom flow (Figs. 2c and 2d), 3) flow with large amplitude of the swaying motion (Fig. 2e), and 4) oscillating vortex pair flow (Fig. 2f). With a further increase of Q (not shown in a figure), the flow pattern became 5) Karman vortexlike flow penetrating upward, which is observed in the heat island plume[11] and the cool plume[12] descending through a stratified layer. Flows 1–5 do not occur in the plume[1–5] in an unstratified ambient and, therefore, characterize the plume in a stratified ambient.

At any Q, the air near the heated wire rises vertically and reaches the plume front, which is the maximum height the fluid reaches on the midplane. Then the fluid near the plume front moves almost horizontally. Thus, a stably stratified ambient covers the plume like a ceiling, and suppresses the plume height, which is the vertical distance from the wire to the plume front. With increasing Q at the given st, the plume height increases as described earlier. A flow

Table 1 Symbols at boundary

Symbol	Interface
▲ ◀	Laminar–transitional
△ ◁	Transitional–turbulent
▽ ▷	Turbulent–retransitional
▼ ▶	Transitional or retransitional-relaminar

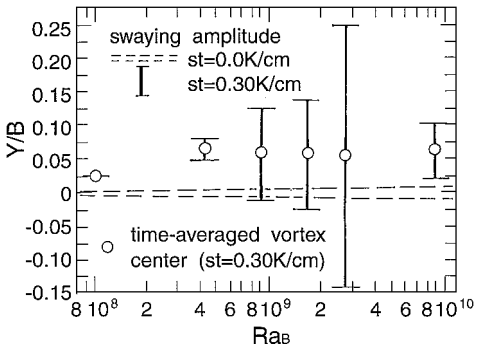

Fig. 3 Amplification of swaying amplitude by stable stratification.

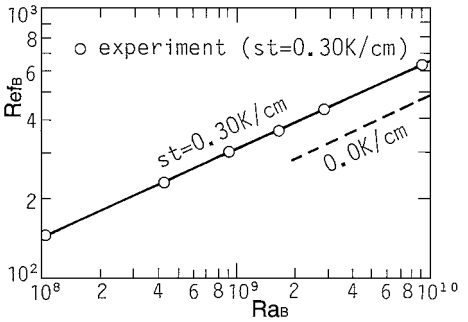

Fig. 4 Increase of swaying frequency by stable stratification.

state cannot be specified by only observing flows 1–4 in Fig. 2. It is specified by the PSDs gradients later. Flow physics of the plume 1–4 is discussed later.

Desrayaud and Lauriat[4] elucidated that the representative length for the plume in an unstratified ambient is not the vertical length between the wire and the ceiling but the horizontal length B. In a stably stratified ambient, because the plume height was suppressed, the representative length also is the length B. The amplitude and the frequency of the swaying motion in a stably stratified ambient were measured by flow visualization and are shown in Figs. 3 and 4. Stable stratification decreases the flow region as seen in Fig. 2 and, as a result, increases the frequency and the amplitude of the swaying motion shown in Figs. 3 and 4. The amplitude becomes small at $5 \times 10^5 < Ra_B$ and is a little larger than that in an unstratified ambient at extremely high Q (Fig. 3). The swaying frequency in a stably stratified ambient can be expressed by Eq. (1) and is compared with Eq. (2) in an unstratified[3,4] ambient.

At $st = 0.3$ K/cm:

$$Re_{fB} = 0.300 Re_B^{\frac{1}{3}} \tag{1}$$

At $st = 0$ K/cm:

$$Re_{fB} = 0.219 Re_B^{\frac{1}{3}} \tag{2}$$

Measured Results

The measured temperature is shown in Figs. 5 and 6a–c and is time dependent near the wire due to only the swaying motion and above the wire due to both turbulence and the swaying motion. The time-averaged temperature, fluctuation intensity (Fig. 7), PDF, and ACC (Fig. 8) were obtained from the time-series data of the

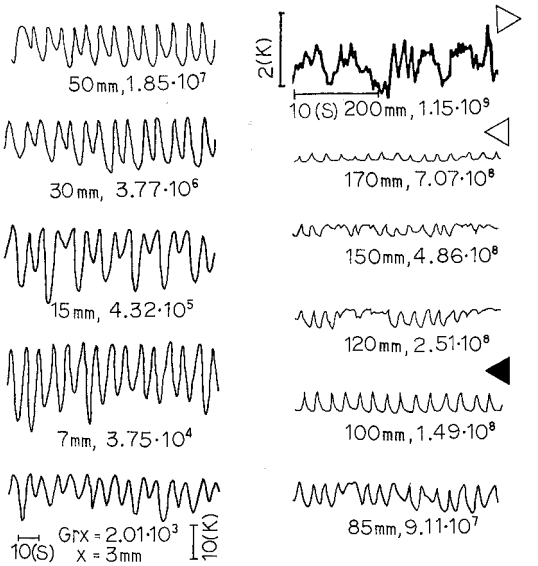

Fig. 5 Time record of temperature on midplane at $st = 0.3$ K/cm and $Q = 27.8$ W/m.

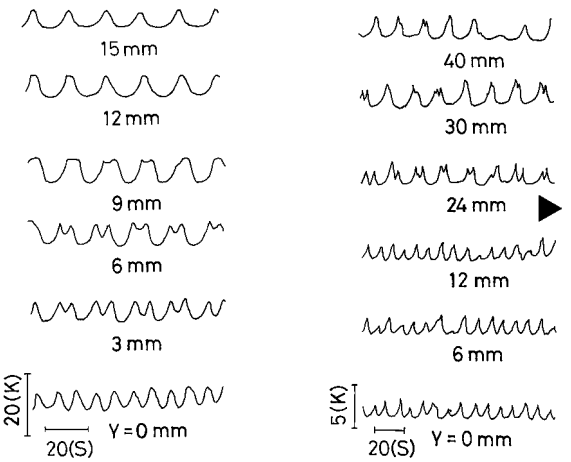

a) Laminar state on midplane at $X = 80$ mm and $Gr_x = 7.77 \times 10^7$

b) Transitional state on midplane at $X = 180$ mm and $Gr_x = 9.02 \times 10^8$

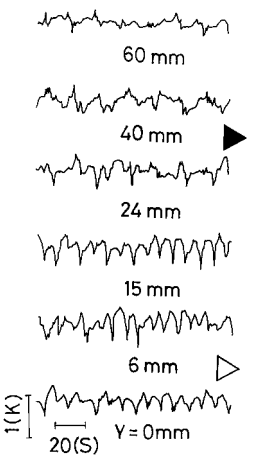

c) Turbulent state on midplane at $X = 220$ mm and $Gr_x = 1.58 \times 10^9$

Fig. 6 Time record of temperature on given height at $st = 0.3$ K/cm and $Q = 27.8$ W/m.

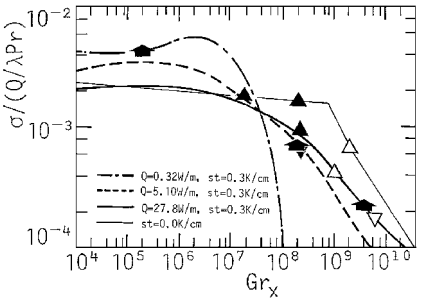

Fig. 7 Temperature fluctuation intensity on midplane due to both turbulence and swaying motion; black arrow shows plume front.

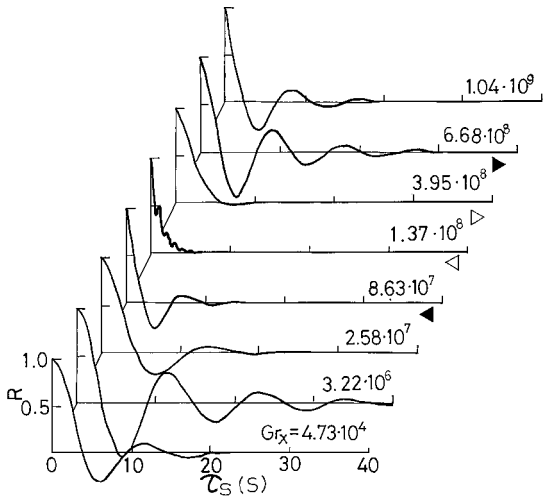

Fig. 8 ACC on midplane at st = 0.3 K/cm and Q = 8.73 W/m.

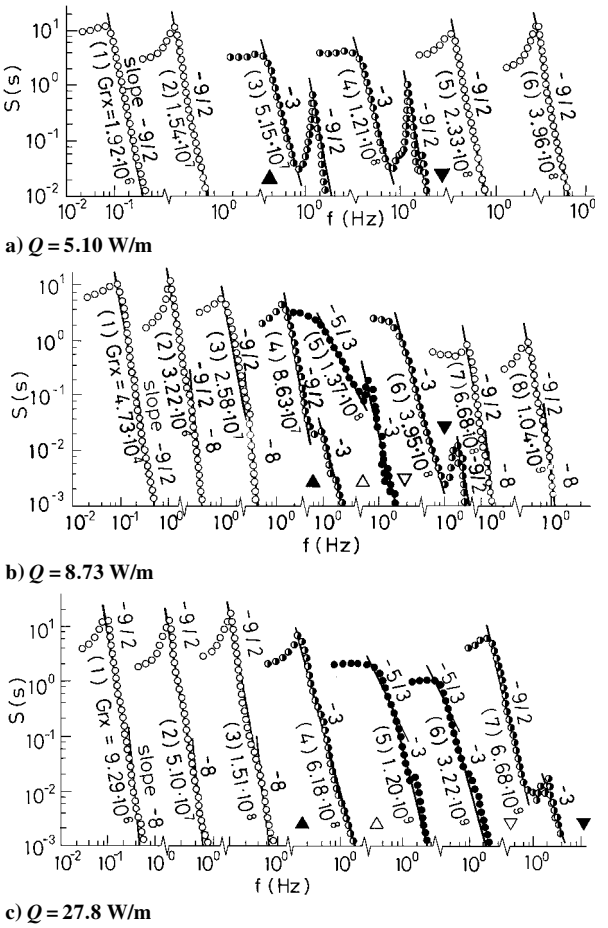

Fig. 9 Spectrum on midplane at st = 0.3 K/cm, where open circle, half-open circle, filled circle, and solid line show laminar, transitional, turbulent, and PSD gradient, respectively.

temperature. Both the turbulence and the swaying motion are occurring simultaneously in every distribution except near the wire, where it is impossible to distinguish clearly between turbulence and the swaying motion and to specify flow states. Flow regions of the laminar, transitional and turbulent states determined by employing the PSD gradients described later are plotted in Figs. 2 and 5–10 using the symbols in Table 1. The flow state on the midplane is shown in Fig. 2, and the region of the turbulent state can be visualized in Figs. 2e and 2f because of a turbulent core with enclosed space, as described later. Distributions in Figs. 5–8 can be explained well by the flow regions as follows: In Figs. 5 and 6, the time-dependent motion in the laminar region near the wire is only due to the swaying motion. A small irregularity due to turbulence occurs in the transitional and the turbulent regions. An intermittent entrainment occurs far away from the midplane, as seen in Fig. 6. In Fig. 7, the plume height, shown by the black arrow, decreases with decreasing Q, and the fluctuation intensity decreases above the plume front by stable stratification. In Fig. 8, the ACC in the laminar region has more correlation than that in the turbulent region, where the turbulent ACC is like a white noise.

PSD and Its Criterion

As shown earlier, the flow state could not be determined by solely observing flow visualization results, the time-record of temperature, fluctuation intensity, PDF, and ACC. The PSD is, therefore, obtained and is discussed for determining the flow state.

PSD and Spectrum Gradient

The PSD S normalized by the temperature variance σ^2 is shown in Figs. 9a–c and 10a–d. The PSD gradient in a diagram of log S–log f had features at $1.30 \leqq Q \leqq 27.8$ W/m as follows: The flow state near the wire is laminar with only the swaying motion, and the PSD gradients are $-\frac{9}{2}$ and -8.0. The laminar PSDs in a stably stratified ambient are shown by the open circles and solid line and are expressed as follows:

$$S[s] \propto \{f\}^{-\frac{9}{2}} \tag{3}$$

$$S[s] \propto \{f\}^{-8.0} \tag{4}$$

The plume far away from the wire has the PSD gradient $-\frac{5}{3}$, which is the same as both Kolmogorov's hypothesis (see Ref. 20) and the theoretical value.[15] The flow state can be regarded as turbulent in the inertia-convective subrange, whose frequency is lower than the inertia-diffusive subrange, where the PSD gradient was found in the present experiment to be certainly -3.0, which is the same as that predicted by Lumley.[15] The turbulent PSDs in a stably stratified ambient, therefore, have gradients $-\frac{5}{3}$ and -3.0 and are shown by the filled circles and solid line and are expressed as follows:

$$S[s] \propto \{f\}^{-\frac{5}{3}} \tag{5}$$

$$S[s] \propto \{f\}^{-3.0} \tag{6}$$

The PSD value with the gradient $-\frac{5}{3}$ is large in the middle of turbulent region in Figs. 9b(5), 9c(5), and 10c, but becomes small in the turbulent region near the boundary with the transitional region as seen in Fig.9c(6). The PSD gradient in the transitional state is between the laminar and the turbulent gradients and is shown by the half open circles and solid line. In PSDs, the swaying frequency defined as the dominant frequency in PSDs agrees well with Eq. (1) and is much lower than that of turbulence with gradient $-\frac{5}{3}$. That is, the swaying motion can be clearly separated from turbulence in PSDs, and the gradients of $-\frac{5}{3}$ and -3.0 in Eqs. (5) and (6) are due to only turbulence.

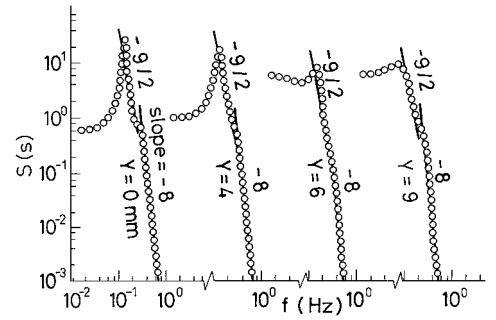

a) Laminar state on midplane at $X = 80$ mm and $Gr_x = 7.77 \times 10^7$

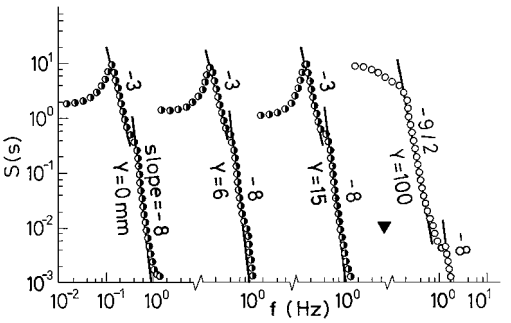

b) Transitional state on midplane at $X = 180$ mm and $Gr_x = 9.02 \times 10^8$

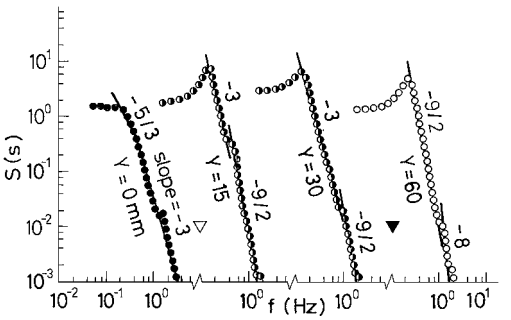

c) Turbulent state on midplane at $X = 220$ mm and $Gr_x = 1.58 \times 10^9$

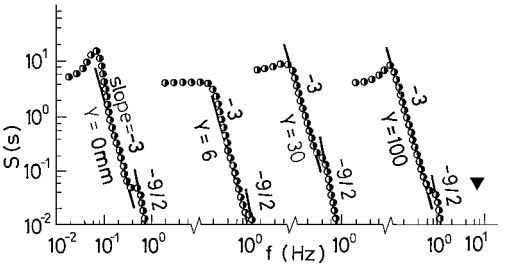

d) Transitional state above turbulent core on midplane at $X = 340$ mm and $Gr_x = 5.70 \times 10^9$

Fig. 10 Spectrum on given height at $st = 0.3$ K/cm and $Q = 27.8$ W/m, where open circle, half-open circle, filled circle, and solid line show laminar, transitional, turbulent, and PSD gradient, respectively.

Criterion for Determining Flow State and Advantage of Present Criterion

A criterion for determining flow states in a stably stratified ambient becomes as follows: Laminar PSDs have the gradients $-\frac{9}{2}$ and -8.0 as in Eqs. (3) and (4), turbulent PSDs have the gradients $-\frac{5}{3}$ and -3.0 as in Eqs. (5) and (6), and the gradients of the transitional state are between the laminar and the turbulent gradients, that is, $(-\frac{9}{2}) \sim (-\frac{5}{3})$ and $(-8.0) \sim (-3.0)$. That is, in the transitional region, the turbulent gradients $-\frac{5}{3}$ and -3.0 depart from the laminar gradients $-\frac{9}{2}$ and -8.0. The 2% departure from the laminar or the turbulent gradients is taken to indicate the two ends of transition.

The PSDs in the laminar and the turbulent states in a stably stratified ambient are found to be the same gradients as those of the plume[3,5] in an unstratified ambient. The criterion in a stably stratified ambient expressed by the gradients is, therefore, the same as that in an unstratified ambient. Furthermore this means that local structures of laminar flow with the swaying motion are very similar between a stratified and an unstratified ambient, and local structures of turbulent motion also are very similar between them. Critical Grashof numbers for the beginning and the end of the turbulent transition on the midplane obtained by the present criterion at $st = 0$ K/cm were nearly the same as the results obtained by other criteria by Forstrom and Sparrow[1] and Bill and Gebhart.[2] The present criterion is, therefore, accurate. However, the existing methods[1,2] for determining flow states are based on qualitative determination and can indicate the beginning and the end of the turbulent transition only on the midplane. Therefore, they cannot be applied to a plume with complicated flow patterns and phenomena, for example, reverse transition and relaminarization. However, the present criterion is based on quantitative determination defined by Eqs. (3–6) and is precise and reasonable. Therefore, it is applicable to any location in the plume in both a stratified and an unstratified ambient. The reverse transition and the relaminarization can be determined by the present method, but cannot be determined by the methods by Forstrom and Sparrow[1] and Bill and Gebhart.[2]

Application of Present Criterion

Flow Region

Flow regions were determined at any location by the present criterion as follows: With increasing X on the midplane at high Q and extremely high Q, the flow state develops to laminar, transitional, turbulent, transitional, and then laminar, as seen in Figs. 9b and 9c. At moderate Q, the laminar flow is transformed to the transitional and the laminar states, but never develops to the turbulent state, as seen in Fig. 9a. Although not shown in a figure, the flow at extremely low Q and low Q is laminar everywhere. As seen in Fig. 10, with an increase of Y from the midplane on the given height, the turbulent state at $Y = 0$ is transformed to the laminar state via the transitional state, and the transitional state at $Y = 0$ is transformed to the laminar state.

Map of Flow Region

Flow regions on the midplane thus determined are shown, indicated by circles at measured locations (Fig. 11), and are compared with those in an unstratified ambient. The plume motion in a stably stratified ambient differs from that of the plume[3–5] in an unstratified ambient, which never develops to transitional or laminar above the turbulent region. Figure 11 is, therefore, very useful to see through plume structures in a stably stratified ambient. The distribution in Fig. 7 is explained well by employing the result in Fig. 11 as follows: The Grashof number Gr_s for the beginning of the turbulent transition decreases with increasing intensity below the plume front. Stable stratification makes the intensity small above the plume front and, therefore, suppresses turbulence.

Application of Flow State to Flow Pattern

The turbulent transition, reverse transition, and relaminarization in a stratified ambient were exactly determined by plotting the flow state and the flow region on the pathline, that is, a locus of a moving particle, in flow visualization results at the conditions of Figs. 9 and 10 and many other conditions and, as a result, were found to occur as described in the following sections.

Turbulent Enhancement

Determination of Beginning and End of Turbulent Transition

The beginning of turbulent transition is defined as follows. The laminar fluid moves, it starts generating turbulence, and then the flow state becomes transitional with turbulence. Here the end of turbulent transition is defined as when the flow becomes turbulent. Whether turbulent transition occurs or not is determined by plotting the flow state on the visualized results. As a result, at low Q, the flow is laminar in every place and never generates turbulence. At moderate Q, the laminar fluid near the wire rises upward, penetrates into the transitional region, and begins turbulent transition, but does not

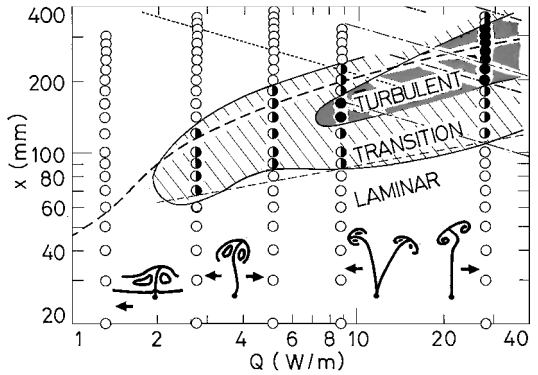

a) X vs Q

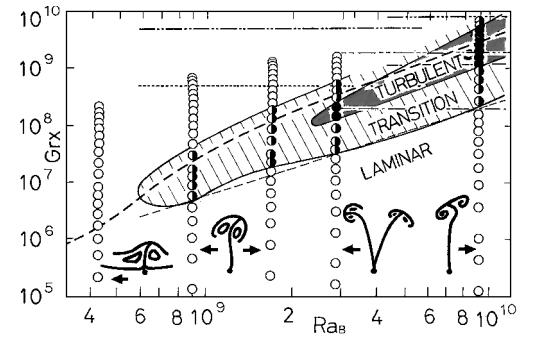

b) Gr_x vs Ra_B

Fig. 11 Regions of laminar state, transitional state, turbulent state, transitional state above turbulent core, and laminar state above turbulent core on midplane at $st = 0.3$ K/cm: – – –, Eq.(7); ——, boundary; - - - -, center of vortex pair; · · · ; beginning of transition at $st = 0$ K/cm obtained by Forstrom and Sparrow,[1]; – – –, beginning of transition at $st = 0$ K/cm obtained by Bill and Gebhart,[2]; – –, beginning of transition at $st = 0$ K/cm obtained by Noto et al.,[5]; – · –, end of transition at $st = 0$ K/cm obtained by Forstrom and Sparrow,[1]; – · · –, end of transition at $st = 0$ K/cm obtained by Bill and Gebhart,[2]; and – - - –, end of transition at $st = 0$ K/cm obtained by Noto et al.[5].

develop to turbulent. At high Q and extremely high Q, the laminar fluid enters the transitional region generating turbulence and then penetrates into the turbulent region. Thus, both the beginning and the ending of turbulent transition occur only at high Q and extremely high Q.

Grashof Number Gr_s for Beginning of Turbulent Transition

In visualized results and Figs. 7 and 11a, the plume front is above the location of the beginning of turbulent transition and becomes low with a decrease of Q. Hence, the Grashof number Gr_s for the beginning of turbulent transition on the midplane in a stratified ambient decreases with decreasing Q as seen in Fig. 11b and can be approximated at $st = 0.3$ K/cm and $4.28 \times 10^8 \leqq Ra_B \leqq 9.15 \times 10^9$ as follows:

$$Gr_s = 1.32 \times 10^8 Ra_B^{1.62} \tag{7}$$

However, the Grashof number Gr_s in unstratified air is independent of Q and is constant, as seen in Fig. 11b. Forstrom and Sparrow,[1] Bill and Gebhart,[2] and Noto et al.[5] obtained $Gr_s = 5.0 \times 10^8$ at $5.83 \times 10^8 \leqq Ra_B \leqq 5.63 \times 10^9$, 1.12×10^9 at $4.28 \times 10^9 \leqq Ra_B \leqq 2.23 \times 10^{10}$, and 2.0×10^8 at $2.87 \times 10^9 \leqq Ra_B \leqq 2.75 \times 10^{10}$.

Enhancement of Turbulent Transition and Its Cause

The Grashof number Gr_s for the beginning of the turbulent state on the midplane in a stratified ambient is smaller than that in an unstratified ambient except at extremely high Q, as seen in Fig. 11. For example, due to stratification, Grashof number Gr_s at $Q = 2.75$ W/m decreases by 96.0%, and turbulent transition begins near the wire. This means that stable stratification enhances the turbulence generation below the plume front, which results from the increases of the swaying amplitude, swaying frequency, and velocity by stable stratification; this has not been reported in previous studies.[13,14] The plume at extremely high Q in stratified air had almost the same swaying amplitude as that in unstratified air as shown in Fig. 3 and, therefore, has almost the same Grashof number Gr_s as the unstratified plume shown in Fig. 11.

Turbulence Suppression

Flow State near Plume Front

The plume height is suppressed by stable stratification as described earlier, and stably stratified air covers the plume like a ceiling. In Fig. 11, the flow in stably stratified air above the plume front is not turbulent, but is transitional or laminar, and covers the turbulent or the transitional regions near the plume front. This means that turbulence is suppressed above the plume front by stable stratification. In other words, the velocity in the X direction decreases above the plume front, where the flow turns to the horizontal direction and moves horizontally consuming turbulent energy as discussed later. Turbulence is, therefore, suppressed near and above the plume front.

Turbulent Core

At high Q and extremely high Q, the turbulent region on the midplane is above and below the transitional regions, as seen in Figs. 9a, 9b, and 11. The turbulent region is beside the transitional state far away from the midplane on the given height as seen in Fig. 10. Thus, the turbulent core is formed and exists near $(X, Y) = (220, 0)$ mm at extremely high Q. Similarly, the transitional core surrounded by the laminar region is formed near the midplane at moderate Q.

Critical Heating Rate

As seen in Fig. 11a, at $st = 0$ K/cm, both the transitional and the turbulent regions occur at $1.77 \leqq Q$ W/m and can be conjectured to occur at $Q < 1.77$ W/m. On the other hand, at $st = 0.3$ K/cm, the transitional and the turbulent regions never occur at low Q, and the turbulent region never occurs at moderate Q. Thus, the critical Rayleigh numbers Ra_{Bs} or Ra_{Be} for either the transition or the turbulent region to occur on the midplane in stable stratification become as follows.

At $st = 0.3$ K/cm:

$$Ra_{Bs} = 4.28 \times 10^8 \sim 9.05 \times 10^8 \tag{8}$$

At $st = 0.3$ K/cm:

$$Ra_{Be} = 1.68 \times 10^9 \sim 2.87 \times 10^9 \tag{9}$$

Summary of Enhancement and Suppression of Turbulence

As described, stable stratification enhances and suppresses turbulence. That is, the flow at $Ra_B < Ra_{Bs}$ is always laminar because of intensive suppression of turbulence and its generation. At $Ra_{Bs} < Ra_B < Ra_{Be}$, turbulence is generated and then suppressed, and the flow never becomes turbulent. At $Ra_{Be} < Ra_B$, turbulence is generated, develops to turbulent below the plume front, and is suppressed above or beside the plume front; then the flow becomes transitional and laminar again.

Reverse Transition and Relaminarization

Determination of Beginning and Ending of Reverse Transition

Generally reverse transition is defined as when turbulence is suppressed and the turbulent fluid is transformed to the transitional state. Relaminarization is defined as when the fluid in the transitional state moves and becomes without turbulence due to turbulence suppression. In the present experiment, the flow region was plotted on the visualized photographs as follows: At extremely low Q and low Q, the flow is laminar everywhere and reverse transition never occurs. At moderate Q, the transitional fluid moves horizontally and then enters the laminar region. Thus, the flow state becomes laminar again, and the reverse transitional process ends. At high Q and extremely high Q, the turbulent fluid enters the transitional region and starts reverse transition. Then the transitional fluid moves

horizontally, penetrates into the laminar region, and begins relaminarization. Thus, stable stratification leads to reverse transition and relaminarization above and/or beside the plume front. This never occurs in the plume[3,5] in an unstratified ambient and characterizes the plume in a stably stratified ambient.

Flow Physics of Reverse Transition and Relaminarization

At high Q and extremely high Q, the fluid heated by the wire rises upward and is always entering the plume front region. Because stably stratified air covers the plume like a ceiling, the fluid motion above the plume front is suppressed by a stably stratified ambient. The turbulent fluid near the plume front with the positive buoyant force, therefore, penetrates barely above the plume front by consuming turbulent energy, and the flow state becomes the transitional state. This is the turbulent suppression and the beginning of the reverse transition. At this time, the flow no longer has a rising force. It then moves horizontally by further consuming turbulent energy, and the flow becomes laminar again. This is relaminarization. Similarly, the turbulent fluid near the plume front without a rising force moves horizontally by consuming turbulent energy and penetrates into the laminar region. At moderate Q, when the fluid of the transitional state with turbulence moves, turbulence is suppressed, and reverse transition begins beside the plume front. Thus, both the transitional and the reverse transitional states exist in the transitional region at only moderate Q. That is, whenever the flow state near the plume front is transitional or turbulent, reverse transition and relaminarization always occur above and/or beside the plume front. Narasimha and Sreenivasan[13] and Tritton[14] indicated the turbulence suppression due to stable stratification but did not reveal the mechanism and its details.

Conclusions

The plume pattern, PSD, criterion, flow state, flow region, turbulent enhancement, reverse transition and relaminarization in the thermal plume in a stably stratified ambient are revealed.

1) Stable stratification suppresses the plume height. With an increase of Q at $st = 0.3$ K/cm, the plume height increases, and the plume pattern is transformed from the fumigation flow to the mushroom flow, then the flow with large amplitude of swaying motion, and the oscillating vortex-pair flow.

2) The plume in a stably stratified ambient has the PSD gradients in the laminar and the turbulent states as follows.

At the laminar state:

$$S[s] \propto \{f\}^{-\frac{9}{2}}, \qquad S[s] \propto \{f\}^{-8.0}$$

At the turbulent state:

$$S[s] \propto \{f\}^{-\frac{5}{3}}, \qquad S[s] \propto \{f\}^{-3.0}$$

The PSD gradient in the turbulent inertia-diffusive subrange is certainly -3.0, which is the same as that predicted by Lumley.[15] Because turbulence has a frequency range larger than that of the swaying motion, the turbulent gradients of $-\frac{5}{3}$ and -3.0 are only due to turbulence. The PSD gradients in the transitional region are between those in the laminar and the turbulent gradients. This is the criterion employing the PSD gradients for exactly determining the flow state. When this criterion is employed, the turbulent transition and the flow regions of the laminar, transitional, and turbulent states can be determined. Furthermore, by employing both the flow region and the pathline on visualized photographs, the turbulent enhancement, turbulent suppression, reverse transition, and relaminarization were able to be specified and characterize the plume in a stably stratified ambient because they never occur in a plume in an unstratified ambient.

3) Critical Grashof number Gr_s for the beginning of turbulent transition on the midplane increases with increasing the Rayleigh number Ra_B at $st = 0.3$ K/cm and $4.28 \times 10^8 \leqq Ra_B \leqq 9.15 \times 10^9$ as follows:

$$Gr_s = 1.32 \times 10^8 Ra_B^{1.62}$$

Critical Rayleigh number at $st = 0.3$ K/cm for the beginning of either the transitional or the turbulent state on the midplane is expressed as follows:

$$Ra_{Bs} = 4.28 \times 10^8 \sim 9.05 \times 10^8$$

$$Ra_{Be} = 1.68 \times 10^9 - 2.87 \times 10^9$$

The plume is always laminar at $Ra_B < Ra_{Bs}$ and always develops to the turbulent state at $Ra_{Be} < Ra_B$.

4) Narasimha[13] and Tritton[14] indicated qualitatively only the turbulence suppression due to stable stratification and did not reveal the mechanism and its details, which can be exactly revealed in the present study.

5) Turbulent enhancement, reverse transition, and relaminarization are not inherent at only the present conditions, that is, $Q = 0.32$–27.8 W/m and $st = 0.3$ K/cm, but are universal phenomena always occurring in a plume in a stably stratified ambient, which can be certainly and exactly revealed by employing the PSDs in the present methods, but cannot be determined by the turbulent burst measured by Forstrom and Sparrow[1] and the Mach–Zehnder visualization by Bill and Gebhart.[2]

References

[1]Forstrom, R. J., and Sparrow, E. M., "Experimental Investigation of Laminar Free-Convection Flow in Air above Horizontal Wire with Constant Heat Flux," *International Journal of Heat and Mass Transfer*, Vol. 10, March 1967, pp. 321–331.

[2]Bill, R. G., and Gebhart, B., "The Transition of Plane Plumes," *International Journal of Heat and Mass Transfer*, Vol. 18, April 1975, pp. 513–526.

[3]Noto, K., "Swaying Motion in Thermal Plume above a Horizontal Line Heat Source," *Journal of Thermophysics and Heat Transfer*, Vol. 3, No. 4, 1989, pp. 428–434.

[4]Desrayaud, G., and Lauriat, G., "Unsteady Confined Buoyant Plumes," *Journal of Fluid Mechanics*, Vol. 252, 1993, pp. 617–646.

[5]Noto, K., Teramoto, K., and Nakajima, T., "Spectra and Critical Grashof Numbers for Turbulent Transition in the Thermal Plume," *Journal of Thermophysics and Heat Transfer*, Vol. 13, No. 1, 1999, pp. 82–90.

[6]Torrance, K. E., "Natural Convection in Thermally Stratified Enclosures with Localized Heating from Below," *Journal of Fluid Mechanics*, Vol. 95, 1979, pp. 477–495.

[7]Giovannoi, J. M., "A Laboratory Analysis of Free Convection Enhanced by a Heat Island in a Calm and Stratified Environment," *Boundary-Layer Meteorology*, Vol. 41, No. 1, 1987, pp. 9–26.

[8]Lu, J., Arya, S. P., Snyder, W. H., and Lawson, R. E., Jr., "A Laboratory Study of the Urban Heat Island in a Calm and Stably Stratified Environment. Part 1: Temperature Field," *Journal of Applied Meteorology*, Vol. 36, No. 10, 1997, pp. 1377–1391.

[9]Lu, J., Arya, S. P., Snyder, W. H., and Lawson, R. E., Jr., "A Laboratory Study of the Urban Heat Island in a Calm and Stably Stratified Environment. Part 2: Velocity Field," *Journal of Applied Meteorology*, Vol. 36, No. 10, 1997, pp. 1392–1402.

[10]Gebhart, B., Jaluria, Y., Mahajan, R., and Sammakia, B., *Buoyancy-Induced Flows and Transport*, Springer-Verlag, Berlin, 1988, pp. 231, 232.

[11]Noto, K., "Dependence of Heat Island Phenomena on Stable Stratification and Quantity in a Calm Environment," *International Journal of the Atmospheric Environment*, Vol. 3, No. 3, 1996, pp. 475–485.

[12]Rast, M. P., "Compressible Plume Dynamics and Stability," *Journal of Fluid Mechanics*, Vol. 369, 1998, pp. 125–149.

[13]Narasimha, R., and Sreenivasan, R., "Relaminarization of Fluid Flows," *Advances in Applied Mechanics*, Vol. 19, No. 2, 1979, pp. 221–309.

[14]Tritton, D. J., *Physical Fluid Dynamics*, 2nd ed., Oxford Univ. Press, Oxford, England, U.K., 1988, pp. 357, 358.

[15]Lumley, J. L., "The Spectrum of Nearly Inertial Turbulence in a Stably Stratified Fluid," *Journal of Atmospheric Sciences*, Vol. 21, No. 1, 1964, pp. 99–102.

[16]Noto, K., and Matsumoto, R., "Swaying Motion in Thermal Plume above a Line Heat Source (Spectral Analysis of Swaying Wave by Means of the MEM)," *Memoirs of Faculty of Engineering*, No. 31, Kobe Univ., Kobe, Japan, 1984, pp. 103–112.

[17]Ulrych, T. J., and Bishop, T. N., "Maximum Spectral Analysis and Autoregressive Decomposition," *Reviews of Geophysics and Space Physics*, Vol. 13, No. 1, 1975, pp. 183–200.

[18]Rouse, H., Yih, C., and Humphreys, H., "Gravitational Convection from a Boundary Source," *Tellus*, Vol. 4, No. 3, 1952, pp. 201–210.

[19]Noto, K., Yamasaki, Y., Ishida, H., and Matsumoto, R., "Swaying Motion of the Buoyant Plume Above a Horizontal Line Heat Source," *Transactions of Japan Society of Mechanical Engineers*, Series B, Vol. 50, 1984, pp. 2179–2188 (in Japanese).

[20]Hinze, J. O., *Turbulence*, McGraw-Hill, New York, 1975, p. 236.